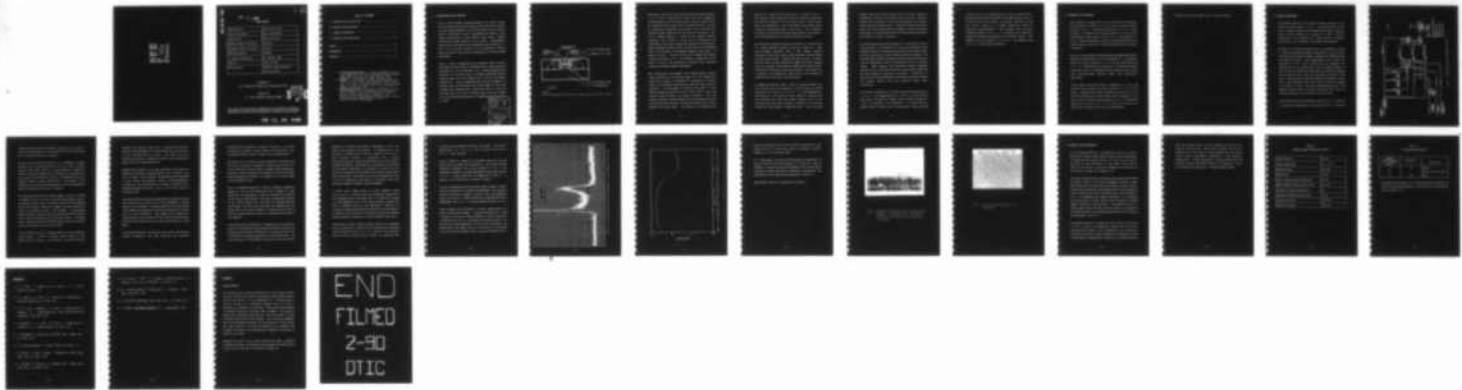


AD-B139 150L

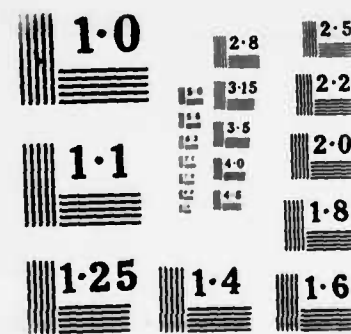
GROWTH OF SEMI-INSULATING INAlAS BY MOCVD(U) ORTEL CORP 1/1  
ALHAMBRA CA J UNGAR 21 OCT 89 DASG60-89-C-0038

EXPORT CTRL  
UNCLASSIFIED

F/G 20/6.1 CTRL



END  
FILED  
2-90  
DTIC



L (2)

DTIC FILE COPY

FINAL REPORT

BMDO Order No.	KE-9-C4269-02-0000
Name of Contractor	Ortel Corporation
Contract No.	DASG60-89-C-0038
Effective Date of Contract	89 APR 21
Expiration Date of Contract	89 OCT 21
Reporting Period	6 Months
Principal Investigator	Dr. Jeffrey Ungar
Phone No.	(818) 281-3636
Title of Work	GROWTH OF SEMI-INSULATING InAlAs BY MOCVD

SPONSORED BY

SDIO INNOVATIVE SCIENCE AND TECHNOLOGY OFFICE

MANAGED BY

U.S. ARMY STRATEGIC DEFENSE COMMAND

DTIC  
ELECTED  
DEC 15 1989  
S D

The views and conclusions contained in this document are those of the authors and should not be interpreted as necessarily representing the official policies, either expressed or implied of the Government.

89 11 08 046

## TABLE OF CONTENTS

1.0 INTRODUCTION AND OVERVIEW .....	1
2.0 RELATED PRIOR RESEARCH .....	6
3.0 GROWTH EXPERIMENTS .....	8
4.0 ANALYSIS AND CONCLUSIONS .....	20
 TABLES .....	22
REFERENCES .....	24
APPENDIX .....	26

- (1) DISTRIBUTION STATEMENT F - Further dissemination only as directed by the U.S. Army Strategic Defense Command, ATTN: CSSD-H-MPL, P.O. Box 1500, Huntsville, AL 35807-3801, 01 Apr 85, or higher DOD authority.
- (2) WARNING - This document contains technical data whose export is restricted by the Arms Export Control Act (Title 22, U.S.C., Sec 2751 et seq.) or Executive Order 12470. Violation of these export laws are subject to severe criminal penalties.
- (3) DESTRUCTION NOTICE - For classified documents, follow the procedures in DOD 5200.22-M, Industrial Security Manual, Section II-19 or DOD 5200.1-R, Information Security Program Regulation, Chapter IX. For unclassified, limited documents, destroy by any method that will prevent disclosure of contents or reconstruction of the document.

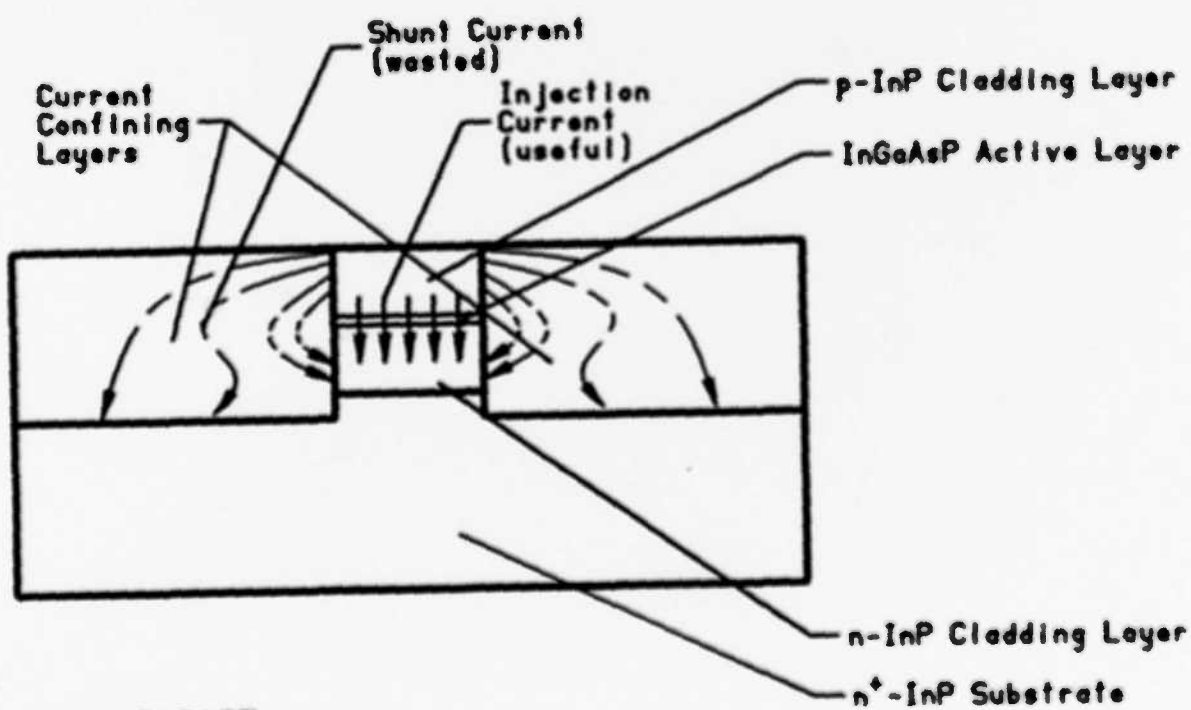
## 1.0 INTRODUCTION AND OVERVIEW

Optical fibers possess strong advantages over coaxial cables for the transmission of high frequency data and signals, because of fiber's high bandwidth, low loss and weight, and its relative immunity to EMP effects and to interception and jamming. Space related applications include phased array radars, antenna remoting and flight controls (fly by fiber). Semiconductor laser diodes fabricated on InP substrates and emitting at 1.3 and 1.55  $\mu$ m are well suited to use as sources for optical fibers, because of the low loss and dispersion of fiber at those wavelengths.

Figure 1 shows a simplified cross sectional view of such a semiconductor laser diode. The diode, which is monolithically fabricated on an InP substrate, has a light-generating core consisting of an active layer of InGaAsP sandwiched between cladding layers of p and n-doped InP on the top and bottom, respectively. Light is generated when the top (p-doped) InP cladding layer is biased positively with respect to the lower (n-doped) InP cladding layer, causing the motion of holes and electrons from the p and n cladding layers into the InGaAsP active layer where they recombine, accompanied by the generation of light.

6/12/82

Accession For	
NTIS CRA&I	<input type="checkbox"/>
DTIC TAB	<input checked="" type="checkbox"/>
Unannounced	<input type="checkbox"/>
Justification	
By	
Distribution	
Availability Codes	
Dist	Avail and/or Special
F-5	\$2.00



U91016Z

Figure 1.

Simplified diagram of InP/InGaAsP laser showing injection and shunt currents.

The width of the active layer must be kept below approximately 2  $\mu m$  in order to selectively excite only the fundamental transverse mode, and the exposed sides of the p-n junction must be covered by single crystal InP or a related material, in order to electrically passivate the junction and to provide the required optical index profile for optical confinement. This InP or related material is known as the current blocking structure, and it plays a crucial role in determining the performance of the laser, because only electrical current which passes through the active layer of the device and recombines there can contribute to the optical output of the laser. As shown in Figure 1, current can also flow through the current blocking structure if it is not perfect, robbing the active layer of current, and resulting in increased laser threshold current and reduced quantum efficiency.

Most conventional InP/InGaAsP laser diodes employ blocking layers consisting of alternating layers of p and n doped InP, where one or several pn junctions are designed to be reverse biased, and therefore nonconducting, when the laser diode is operating. The performance of devices using only a single reverse biased pn junction is poor, and so two or more such reverse biased junctions are usually necessary. Even with several junctions, current leakage still occurs because current can flow from the p cladding, through the blocking layer located opposite the active layer, and re-enter the n cladding layer

without ever entering the active layer, as shown in Fig. 1. The leakage current through pn junctions rapidly worsens when the operating temperature of the laser diode is significantly above room temperature. Most InP/InGaAsP laser diodes cannot operate at temperatures near or above 100°C. This limitation is serious for space and military applications, and diodes in such environments must be thermo-electrically cooled.

An alternative blocking structure consists of a single layer of a highly resistive material such as Fe doped InP. Such semi-insulating materials offer a much simpler blocking structure and are more easily fabricated than reverse biased pn blocking structures. Because the entire layer is nonconducting, shunt currents between the upper and lower cladding layers are reduced. The parasitic capacitance of such layers, which must be minimized in high speed devices, can be very low. In addition, the temperature sensitivity of the blocking is expected to be lower than for pn blocking.

Fe doped InP blocking layers, which are grown by MOCVD, can have resistivities (as measured by Van der Pauw or related techniques) as high as  $2 \times 10^9 \Omega\text{-cm}^{-3}$  at room temperature. Unfortunately, in an operating laser, holes are injected into the blocking layer from the p-type cladding layer as are electrons from the n-type cladding, resulting in an effective resistivity many orders of magnitude lower. This so-called

"double injection" effect becomes worse at higher operating temperatures, because more electrons and holes are thermally excited over the potential barriers that separate the cladding layers from the blocking layer. A desirable blocking material should have the highest possible bandgap in order to maximize the height of these potential barriers and therefore minimize the effects of carrier injection.

An additional problem arises because Fe is a poison for active layer material, and therefore if Fe has been introduced into an MOCVD reactor to grow blocking structures, the reactor cannot be used to grow active layers without extensive cleaning. Two separate MOCVD systems are generally used to grow these devices, with one dedicated to active structures and one to blocking layers. MOCVD systems with associated support equipment generally cost of the order of \$500,000, and structures requiring two such systems are expected to be costly. In addition, Fe doped InP contains precipitates of FeP which introduce stresses and crystal defects which may adversely affect laser reliability.

An alternate candidate for a single layer blocking material is  $In_{0.53}Al_{0.47}As$ . Its bandgap energy of 1.460 eV is 110 meV greater than that of Fe doped InP layers, and its lattice constant of 5.867 Å is matched to InP substrates. A related material, GaAlAs, which is widely used in semiconductor lasers emitting

in the 0.8-0.85  $\mu m$  wavelength range, can be rendered semi-insulating when grown with MOCVD by introducing ppm levels of O<sub>2</sub> into the source gas stream. By contrast, GaAs can be grown with similar levels of O<sub>2</sub> without significant change in electrical characteristics. This suggests that the semi-insulating nature of O<sub>1</sub>Ge<sub>1-x</sub>Al<sub>x</sub>As is related to an interaction between the Oxygen and Aluminum in the crystal lattice. This argument can be extended to In<sub>x</sub>Al<sub>1-x</sub>As, and suggests that O<sub>1</sub>In<sub>x</sub>Al<sub>1-x</sub>As may be semi-insulating.

## 2.0 RELATED PRIOR RESEARCH

Semi-insulating Fe doped InP was first grown using atmospheric pressure MOCVD by Long et al [1] and using low pressure MOCVD by Hess et al [2]. Resistivities as high as  $2 \times 10^8 \Omega\text{-cm}$  were obtained. The presence of FeP precipitates in Fe:InP has been investigated, among others, by Chu [3] et al and Nakahara et al [4]. These precipitates introduce stress concentrations and crystal defects in the InP [5] which may adversely affect device reliability.

The role of oxygen doping in GaAlAs grown by atmospheric pressure MOCVD was investigated by Terzo and Szwarcow [6]. Low pressure MOCVD was used by Okayasu et al [7] to grow semi-insulating Ga<sub>x</sub>Al<sub>1-x</sub>As. Resistivities as high as  $10^8 \Omega\text{-cm}$  were obtained and short wave (0.85  $\mu\text{m}$  wavelength) buried heterostructure lasers with semi-insulating blocking layers were successfully fabricated.

Liquid phase epitaxy was used by Tanahashi et al [8], and molecular beam epitaxy was used by Davies et al [9] to grow InAlAs. MOCVD was first used by diPonte-Poisson et al [10] to grow not-intentionally doped InAlAs lattice matched to InP. Lower residual electron concentrations ( $7 \times 10^{15} \text{ cm}^{-3}$ ) and electron mobilities as high as  $4482 \text{ cm}^2/\text{V}\cdot\text{s}$  were later reported for MOCVD grown undoped InAlAs by Ains and Mettingly.

OITALAS has not been grown prior to present program.

### 3.0 GROWTH EXPERIMENTS

Low pressure MOCVD was the growth technique adopted for the growth of Oxygen doped  $In_xAl_{1-x}As$ . The growths were carried out in a commercial Encore CS 3200 MOCVD growth system. Epitaxial growth occurs through the reaction of alkyl molecules containing, in the present case, either Indium or Aluminum, with Arsine ( $AsH_3$ ) molecules over heated InP substrate.

The gas flow through the MOCVD system is diagrammed in Figure 2. Hydrogen gas passes through a Palladium cell purifier after which accurately metered amounts of Hydrogen are bubbled through the group III alkyls. The temperatures of the alkyls are regulated to 0.1°C. After leaving the alkyl bubbler, the carrier gas can be valved either into the growth chamber or into a vent line. Whatever the destination, additional hydrogen gas is supplied from a mass flow controller in order to build up to a back pressure of several hundred torr against a needle valve. The pressures in the alkyl and vent lines are adjusted to be equal, in order to keep the downstream pressure on the bubbler constant and to minimize transients when alkyls are switched between the alkyl growth and vent lines.

The Aluminum source was trimethyl Aluminum ( $(CH_3)_3Al$ ), which is a liquid at room temperature (melting point 15.4°C). The Indium

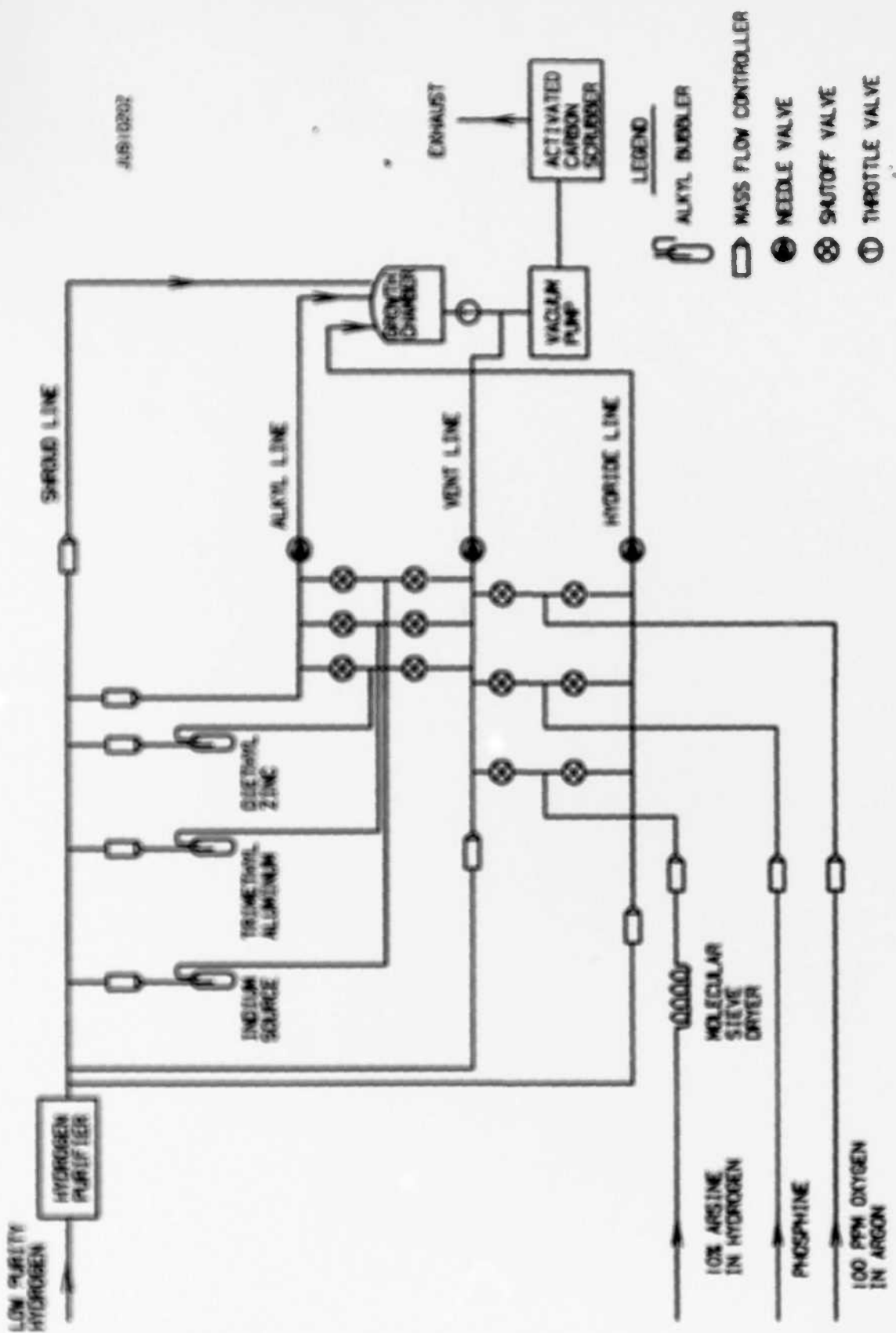


Figure 2. Simplified diagram of MOCVD growth system.

source originally used was TriMethyl Indium ((CH<sub>3</sub>)<sub>3</sub>Al), which is a solid at room temperature (melting point 88°C) but nevertheless has a relatively high vapor pressure.

Arsine, which is supplied diluted 9 to 1 in Hydrogen, is passed through a coil containing molecular sieve in order to remove residual water vapor, which is a common impurity in commercial arsine. The oxygen dopant, which is supplied at a concentration of 100 ppm in ultra high purity Argon, and Phosphine (100%) are supplied without further purification. The purpose of the Phosphine is to retard thermal decomposition of the InP substrate during the heat-up cycle prior to growth.

The reactant gases flow into growth chamber, which is 10 inches in diameter and of cold wall stainless steel design, through perforated injector tubes. An overall "shroud" flow of Hydrogen which flows through a perforated chamber top plate defines the overall flow pattern of gas in the chamber. A vacuum pump, acting through an automatically controlled throttling exhaust valve, keeps the pressure at the desired set point. The vacuum pump is exhausted into an activated carbon filter which removes arsine and phosphine from the gas stream.

The InP substrate sits in a recessed groove in a flat Molybdenum wafer carrier 5 inches in diameter which rotates at 1500 revolutions per minute. The rotation of the wafer carrier

entrains the reactant gases into a rotating flow pattern, enhancing the homogeneity of the gas composition and uniformity of the resulting epitaxial layers. The wafer carrier is resistively heated by a graphite filament and the temperature stabilized by a thermocouple probe.

Growths were carried out on semi-insulating Iron doped InP substrates (supplied by Nippon Mining, Inc.) oriented in the  $(100) \pm 2^\circ$  plane. Prior to growth, the substrates were degreased in warm acetone and methanol, etched in Bromine-methanol, followed by a free surface etch in a mixture of sulfuric acid, hydrogen peroxide and water (3:1:1), and a final rinse in deionized water.

The resistivities and carrier concentrations in epitaxial layers were measured by the Hall-Van der Pauw technique on cleaved squares 1 cm in diameter. Contact was made to the four corners of the sample with Indium dots, which were alloyed to the surface under an inert atmosphere. Some samples were additionally characterized using a Bio-Rad PW 4200 Polaron electrochemical profiler, which provides a plot of carrier concentration versus depth.

Surface morphology was evaluated by both optical and scanning electron microscopy, and layer thickness and thickness

uniformity were measured by chemical staining of the layer followed by microscopy. Lattice constant of the epitaxial layer was measured using a double crystal x-ray diffractometer.

The atomic size of Gallium is almost identical to Aluminum, and the ratio of Gallium to Aluminum in GaAlAs can be varied over a wide range with little change in MOCVD growth properties. Therefore, growth conditions were chosen to be similar to those used successfully by others (e.g. Razeghi [12]) to grow InGaAs lattice matched to InP.

Prior to attempting growth of InAlAs, separate calibration growths of InP (on InP substrates) and of GaAlAs (on GaAs substrates) were performed, in order to determine the relative growth rates of InP and GaAs. The ratio of Aluminum to Gallium in the GaAlAs growths was evaluated by photoluminescence spectroscopy, and the data was analyzed by assuming that the growth rate of the InAs component of InAlAs was the same as that for InP when identical amounts of Indium precursor material are supplied.

Good growth rates (1000 Å/minute), reproducibility, and material quality (as indicated by strong photoluminescence emission) was obtained from the GaAlAs calibrations, but great difficulty was encountered in achieving reasonably high growth rates. The vapor pressure of the TriMethyl Indium was raised as high as

possible by increasing the bubbler temperature to 60°C, but growth rates remained  $\leq$  80 Å/minute. At temperatures of 40°C and above, Trimethyl Indium, which is supplied in the form of small granules, begins to crystallize into a single polycrystalline mass, which does not permit gas to flow properly through the bubbler. The formation of this mass is accelerated as the bubbler temperature is increased, and sufficient flow could be maintained only by mechanically agitating the bubbler after each growth. The growth rate varied irreproducibly from run to run, depending on the degree of agitation, and it was decided to abandon TriMethyl Indium altogether.

A lesser known Indium source is Ethyl DiMethyl Indium ( $(CH_3)_2(C_2H_5)In$ ). Extensive data on the physical properties of this compound are not available, but it is known to be liquid at room temperature and to have vapor pressure roughly half that of TriMethyl Indium at room temperature. Because it is a liquid, problems associated with crystallization are absent. In addition, the liquid nature of the alkyl ensures that hydrogen passing through the bubbler is highly saturated with vapor.

Substitution of Ethyl DiMethyl Indium resulted in an immediate jump in growth rate. A growth rate of 100 Å/minute was obtained with the bubbler held at 27°C. As a check on the electrical quality of the InP grown with this source, an n-type InP layer

was grown using Hydrogen Selenide as the dopant. An electron concentration of  $1.5 \times 10^{19} \text{ cm}^{-3}$  and an electron mobility of  $900 \text{ cm}^2/\text{V}\cdot\text{s}$  was obtained.

Initial growths of InAlAs were performed using the InP and GaAlAs data as growth rate calibrations. The initial growth resulted in material with lattice mismatch of  $1.8 \times 10^{-2}$ , and subsequent refinement of growth parameters reduced the mismatch to  $6 \times 10^{-3}$ . Growth conditions are summarized in Table I. A typical x-ray rocking curve is shown in Figure 3.

In order to demonstrate that the InAlAs could be doped, a growth with Zn introduced as a p-dopant was performed. The resulting material was heavily p-doped, as shown in the electrochemical profile of Figure 4. The hole mobility as determined by Hall measurement, was  $70 \text{ cm}^2/\text{V}\cdot\text{s}$  and the resistivity was  $0.14\Omega\text{-cm}$ .

InAlAs growths were performed at several concentrations of Oxygen in the growth chamber. A growth performed with 0.2 ppm of Oxygen in the source stream resulted in a smooth layer with a resistivity of  $20\Omega\text{-cm}$ . Increasing the Oxygen content to 0.4 ppm did not cause degradation of the surface smoothness, but unfortunately the sample came out non-uniform, as determined by the Van der Pauw system, and an accurate determination of

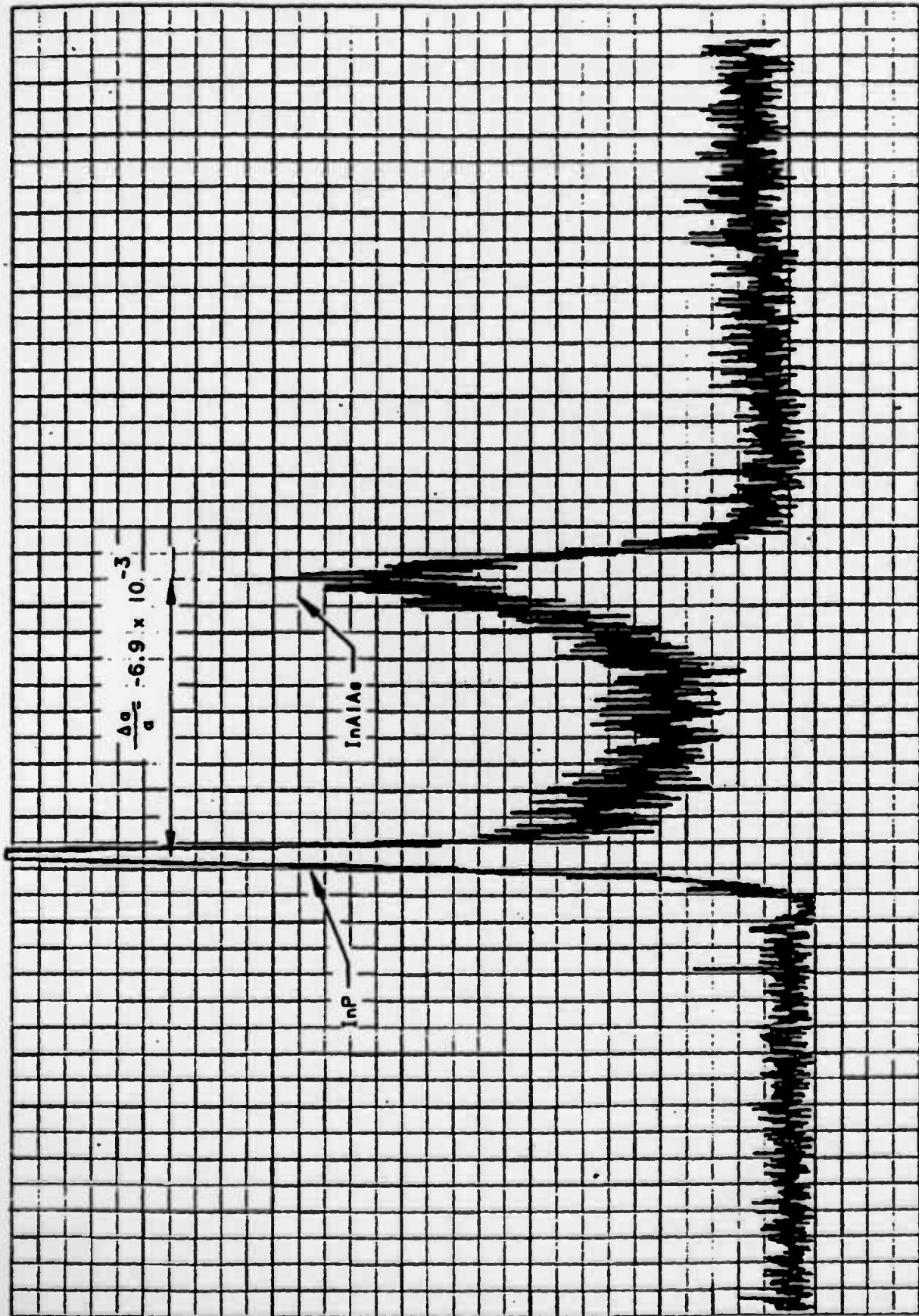


Figure 3. X-ray rocking curve of InAlAs on InP substrate. Lattice mismatch is  $-6.9 \times 10^{-3}$ .

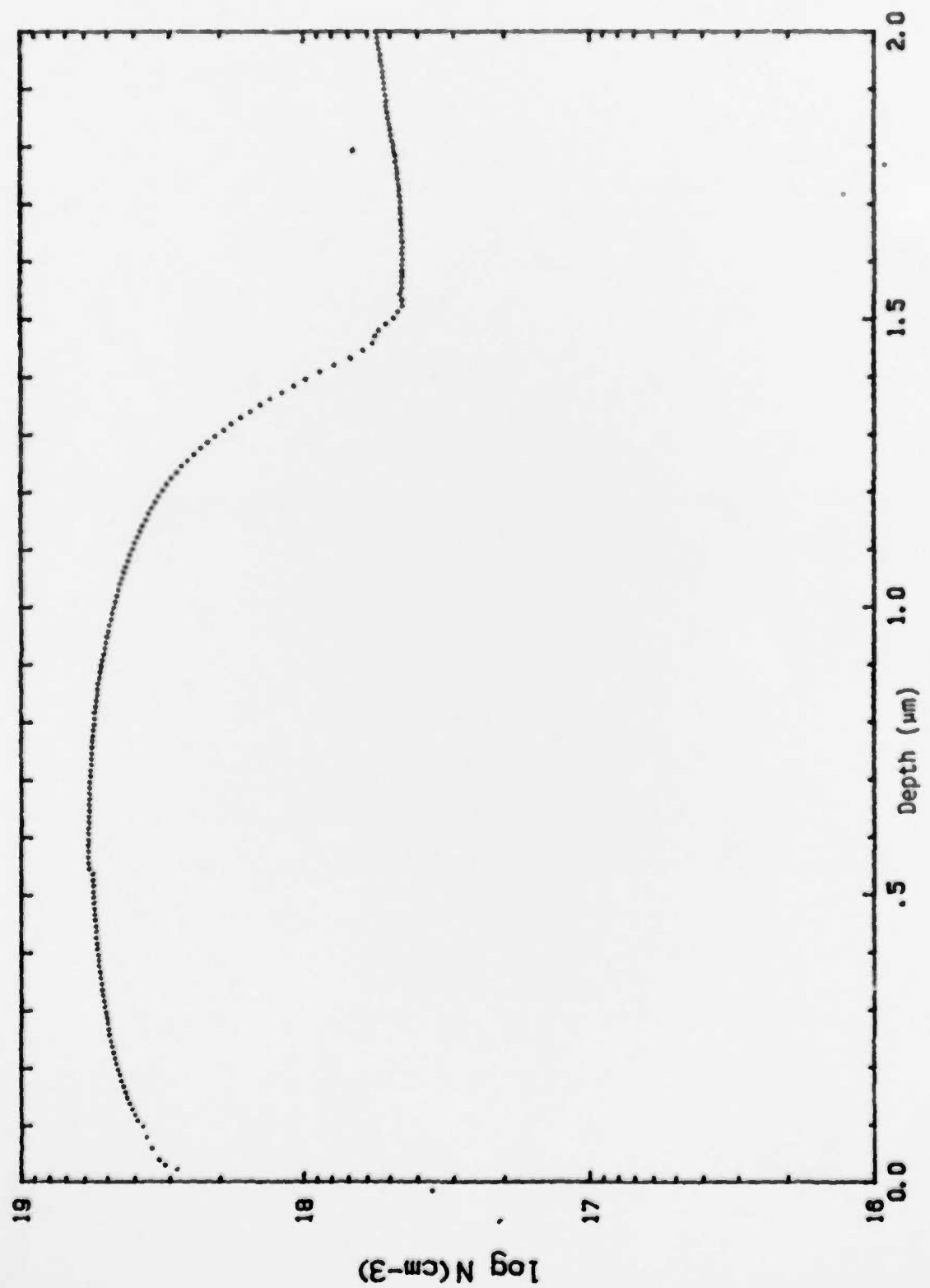


Figure 4. Electrochemical profile of hole concentration versus depth for Zn doped InAlAs.

material resistivity could not be obtained. Examination of the sample with an I-V curve tracer gave an estimate of several hundred  $\Omega\text{-cm}$  for the resistivity.

At 0.7 ppm Oxygen, the surface became milky in appearance, as shown in Figure 5 where the surfaces at 0.4 ppm and 0.7 ppm are compared. A scanning electron micrograph of the surface shown in Figure 6 reveals significant roughening of the surface. The resistivity of the material was measured at  $1200\Omega\text{-cm}$ .

These growth results are summarized in Table II.

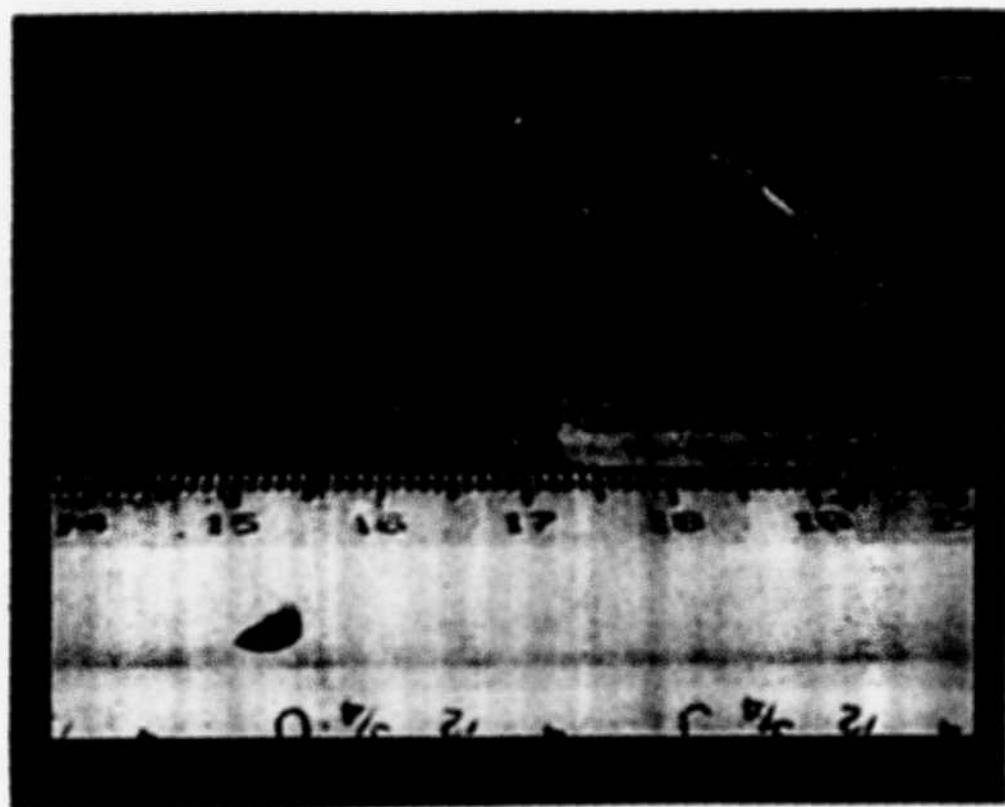


Figure 5. Appearance of InAlAs grown with 0.4 ppm Oxygen (left) compared to 0.7 ppm Oxygen (right). Note specular appearance of 0.4 ppm sample and milky appearance of 0.7 ppm sample.



Figure 6. Scanning electron micrograph of 0.7 ppm Oxygen InAlAs.

#### 4.0 ANALYSIS AND CONCLUSIONS

We have demonstrated that, as predicted by analogy to GaAlAs, MOCVD grown InAlAs becomes highly resistive upon incorporation of Oxygen into the crystal lattice. As is the case for GaAlAs, the onset of high resistivity is very rapid; in the case of InAlAs, we have seen a sixty-fold increase of resistivity for an increase of Oxygen by a factor of 3.5.

The growth conditions that we explored gave rough surfaces when the Oxygen content in the growth atmosphere exceeded 0.7 ppm. Rough surfaces are indications of poor material quality and are not directly suitable for device applications, and so the highest useful resistivities that we obtained were in the hundreds of  $\Omega\text{-cm}$ . By optimizing the growth conditions, it is expected that good material surface quality can be obtained at higher Oxygen contents and resistivities. The material quality of Oxygen doped GaAlAs has been similarly shown to be sensitive to growth conditions, as evidenced by different results reported by References (6) and (7).

The competing material, Fe doped InP, has a resistivity of order  $2 \times 10^5 \Omega\text{-cm}$ , which is considerably greater than the results obtained from O:InAlAs, but as explained in the introduction and Overview section, direct comparison of resistivity values is meaningless, because double injection of electrons and holes

into the blocking layer from the claddings gives far lower effective resistivities. The effects of double injection are expected to be less severe in high bandgap InAlAs and should provide superior performance, especially at high operating temperatures. Further experiments, including fabrication and testing of actual InP/InGaAsP lasers are necessary to verify the performance advantages of 0.15InAlAs blocking layers.

Table I  
Typical Growth Conditions, InAlAs

Growth Pressure	30 torr
Growth Temperature	550 - 650°C
Rotation Speed	1500 RPM
Shroud Flow	12 LPM
Dibutyl Dimethyl Indium Temperature	25-40°C
Dibutyl Dimethyl Indium Carrier Flow	100 cm
Trimethyl Aluminum Temperature	36°
Trimethyl Aluminum Carrier Flow	6 cm
ArSine (10%) Flow	1000 cm
Bubbler Pressures	300 torr

Table II  
O<sub>3</sub> InAlAs Characteristics

Oxygen Concentration in Growth Chamber (ppm)	Resistivity (Ω-cm)	Morphology
0.2	20	Smooth
0.4	*	Linear surface features
0.7	1200	Milky

\* The sample was anisotropic and no reliable figures could be derived from Van der Pauw measurements. The resistivity is estimated at several hundred Ω-cm.

## REFERENCES

1. J. J. A. Long, V. G. Biggs and W. D. Johnston, Jr., *J. Crystal Growth*, **62** (1982), 10.
2. K. K. Kim, S. W. Kim, K. H. Chang and D. Parvezkhan, *J. Electronic Materials*, **16** (1987), 127.
3. S. N. G. Chu, S. Nakamura, J. J. A. Long, V. G. Biggs and W. D. Johnston, Jr., *J. Electron. Solid-State Science and Technology*, **132** (1985), 2795.
4. S. Nakamura, S. N. G. Chu, J. J. A. Long, V. G. Biggs and W. D. Johnston, Jr., *J. Crystal Growth*, **72** (1985), 693.
5. T. Tanahashi, K. Nakai and K. Nakajima, *Rep. J. Appl. Phys.*, **22** (1983), 5413.
6. H. Terao and Suzuki, *J. Crystal Growth*, **58** (1982), 157.
7. M. Okayasu, S. Kotera, Y. Suzuki, J. Tomono and S. Uehara, *Appl. Phys. Lett.*, **51** (1987), 1980.
8. T. Tanahashi, K. Nakajima, A. Yamaguchi and T. Ono, *Appl. Phys. Lett.*, **43** (1983), 1038.

9. G. J. Davies, T. Kerr, C. G. Tuppen, B. Wakefield and D. A. Andrews, *J. Vac. Sci. and Technol.*, B2 (1984), 219.

10. H. A. diPerte-Poisson, M. Raseghi and J. P. Duchemin, *J. Appl. Phys.*, 54 (1983), 7147.

11. L. Aina and W. Mettingly, *Appl. Phys. Lett.*, 51 (1988), 1637.

12. M. Raseghi, *The NOCTD Challenge*, Vol. 1, Adam Hilger, 1989.

## **APPENDIX**

### **Safety Hazards**

The primary safety hazards associated with this program concerns the use of highly toxic gases in the MOCVD crystal growth process, in particular Arsine ( $AsH_3$ ) and Phosphine ( $PH_3$ ). The more toxic of the two, Arsine, has a government required limit of 50 ppb in breathing air, based on an 8 hour/day. The growth system exhaust is filtered through an activated carbon scrubber. The resulting exhaust was continuously monitored by a toxic gas sensor to ensure the proper functioning of the scrubber. The laboratory atmosphere was also continuously monitored for the presence of toxic gases. The source bottles of Arsine and Phosphine were equipped with pneumatic shut-offs to be automatically triggered in the event of detection of toxics.

Hydrogen was used in the growth process and posed a possible flammability hazard. The laboratory was equipped with sensors wired to shut off all gas flow in the event of detection.

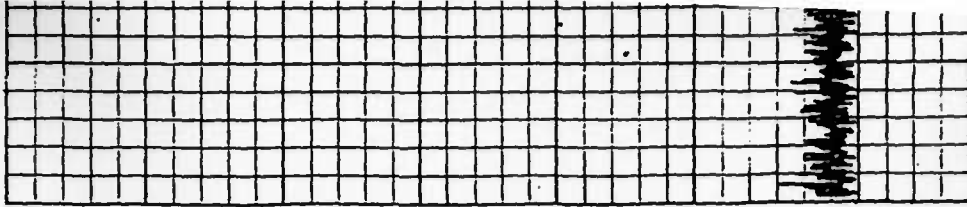
END

FILMED

2-90

DTIC

by the Van der Pauw system, and an accurate determination of



Fig

- 16 -

7. K. Okuyama, S. Kozai, Y. Harada, J. Tomono and S. Ichihara, Appl.  
Phys. Lett. 51 (1987), 1980.

8. T. Tanahashi, K. Nakajima, A. Yamaguchi and T. Onabe, Appl.  
Phys. Lett., 43 (1983), 1030.



- 27 -

DTIC